ELSEVIER

Journal of Photochemistry and Photobiology A: Chemistry 119 (1998) 123–135

Journal of Photochemistry and Photobiology A:Chemistry

Laser desorption ionization of gramicidin S on thin silver films with matrix isolation in surface plasmon resonance excitation

Sandy Owega, Edward P.C. Lai*, Wayne M. Mullett

Department of Chemistry, Ottawa-Carleton Chemistry Institute, Carleton University, Ottawa, Ont., K1S 5B6, Canada

Received 2 March 1998; accepted 18 August 1998

Abstract

Laser desorption ionization (LDI)/laser ablation (LA) time-of-flight mass spectrometry (TOFMS) studies are performed via back-illumination on thin silver films deposited with gramicidin S, a cyclic decapeptide (1141 Da). Experimental results indicate an electronic excitation mechanism at low laser fluences and a thermal process at high laser fluences. In a perpendicular orientation of the thin silver film with respect to the drift tube axis, better success of chemical ionization (CI) of neutral silver atoms/clusters and gramicidin S molecules by Ag^+ monomer cations within the ablation plume is evident. When these LDI/LA studies are repeated under surface plasmon resonance (SPR) conditions, the neutral atoms/clusters/molecules undergo SPR LDI/LA via a different laser energy transfer process compared to direct LDI/LA. These results also indicate an electronic excitation mechanism, only with a lower laser fluence requirement. Upon addition of a matrix, 2,5-dihydroxybenzoic acid (DHB), CI of gramicidin S molecules by Ag^+ monomer cations is hindered while the CI of gramicidin S molecules by Na^+ cations can occur at an even lower laser fluence. Thus, SPR LDI/LA with matrix isolation is an excellent technique for the mass analysis of gramicidin S.

Keywords: Laser desorption ionization; Time-of-flight mass spectrometry; Matrix isolation; Surface plasmon resonance; Silver film substrate; Chemical ionization; Electronic excitation mechanism

1. Introduction

Since the early introduction of laser desorption ionization (LDI) of neutral peptide molecules on an organic substrate [1], attention has been focused on the LDI mechanism to improve analytical performance. An essential process among the variety of laser substrate interactions is the non-thermal desorption of atoms, ions and molecules from the surface of metals during laser ablation (LA) [2–4], although the influence of thermal diffusion on threshold fluences has been demonstrated [5–8]. Non-thermal LDI/LA is induced by the absorption of 355 and 532 nm wavelengths, which results in an electronic transition to an anti-bonding orbital [9], while a 1064 nm wavelength cannot reach the anti-bonding energy (due to its lower photon energy) and therefore a thermal pathway is preferred. During this electronic transition, atoms and molecules are preferentially desorbed from defects of the surface, i.e., from sites with particularly low coordination numbers [10–14]. The relative number of such defect sites can be varied intentionally by changing the size and shape of clusters grown in the substrate preparation [9].

Substrates, including metals, used in LDI/LA investigations have decreased the internal energy of analyte molecules, thereby reducing fragmentation by an order of magnitude [15]. Depending on the electronic nature of metal substrates, different types of gas-phase reactions are promoted for different analytes [16–21]. It has recently been reported that certain metal cation products can act as chemical ionization (CI) reagents [22–29]. During CI, the production of cluster cations have also been observed in the mass spectra [22,23,28,30].

The influence of surface plasmon resonance (SPR) on the LDI/LA mechanism has also been investigated [31,32]. For a given level of ablation damage in a particular film, the fluence required by the SPR technique is 3–5 times less than that needed when direct illumination is used [33,34]. The SPR LDI/LA process involves an electronic excitation mechanism, which is a non-thermal desorption path [9,28,31–33]. This low-fluence excitation technique preserves the integrity of molecular ions, thereby simplifying mass analysis.

*Corresponding author. +1-613-520-2600-3835; fax: +1-613-520-3749; e-mail: edward_lai@carleton.ca

1010-6030/98/$ – see front matter
PII: S1010-6030(98)00397-9

In this paper, we present different approaches of studying the LDI/LA process by orienting thin silver films parallel or perpendicular to the drift tube axis of a TOFMS spectrometer. Experiments using different thin silver film surfaces are performed with and without the deposition of a cyclic decapeptide, gramicidin S. In addition LDI/LA mechanisms with and without SPR excitation are investigated. Lastly, a matrix compound 2,5-dihydroxybenzoic acid (DHB) [35,36], which has been successfully tested with gramicidin S in previous MALDI research [37], is used to investigate the matrix isolation effect under SPR excitation conditions for the first time.

2. Experimental

2.1. Thin silver films

The Lumonics Optics Group (Nepean, ON) prepared thin silver films by thermal evaporation of 99.9% pure silver at a base pressure of 10^{-7} torr and deposition on one clean face of microscope glass slides. Their nominal thicknesses, given by a quartz crystal oscillator in the evaporation system, were 40 nm. They were stored in a vacuum dessicator until use.

2.2. Chemicals

HNO_3, NaOH, NH_4OH, $AgNO_3$, benzaldehyde, and 2,5-dihydroxybenzoic acid (DHB) were purchased from Aldrich (Milwaukee, WI). Gramicidin S hydrochloride was obtained from Sigma (St. Louis, MO). HPLC-grade acetone, methanol and ethanol were purchased from Caledon (Georgetown, ON). All chemicals were used without further purification or treatment.

2.3. Tollen's thin silver films

Microscope glass slides and a Pyrex petri dish were cleaned with acetone, soaked in 100% HNO_3 for 2 days, boiled in the HNO_3 for 1 h, and rinsed with distilled deionized water. In the clean petri dish, 1 ml of 10% NaOH was added to 40 ml of 5% $AgNO_3$ to produce the brown Ag_2O precipitate. The solution was diluted with 150 ml distilled deionized water before the precipitate was dissolved in a minimum amount ($\sim$3 ml) of 50% NH_4OH, added dropwise while the solution was being stirred. 0.1 ml of benzaldehyde was added, and the reaction mixture was quickly stirred. Several clean glass slides were positioned in this Tollen's reagent solution for silver plating after the petri dish was placed on a hot plate set at 50°C. At various times, the silver-coated glass slides were removed from the plating solution and rinsed with distilled deionized water. After drying in air, these Tollen's thin silver films were stored in a vacuum dessicator until use. Before these films were used, each was analyzed by a UV-Vis spectrophotometer to determine its silver film thickness. Note that Tollen's reagent solution on standing has the capability of forming silver fulminate ($AgC_2N_2O_2$), which is a violently explosive compound. Prepare the Tollen's reagent solution immediately before use and dispose of the solution into a waste container with plenty of water immediately after plating.

2.4. Gramicidin S sample preparation

A 50 μl aliquot of 4.5 mg ml^{-1} gramicidin S solution in methanol was deposited on a 2.5 × 2.5 cm^2 Lumonics or Tollen's thin silver film and air dried. The dry sample was placed inside the ion source chamber of a TOFMS spectrometer for LDI/LA analysis. Before the dry sample was analyzed by SPR LDI/LA TOFMS, a SPR angular profile was taken to ensure that SPR activity existed. For SPR LDI/LA TOFMS analysis in the presence of a matrix, a 250 μl aliquot of 0.2 mg ml^{-1} gramicidin S solution in methanol and a 250 μl aliquot of 10.0 mg ml^{-1} DHB solution in ethanol were deposited on a 2.5 × 2.5 cm^2 Lumonics thin silver film and air dried.

2.5. Laser desorption ionization/laser ablation

The second harmonic ($\lambda = 532$ nm) output of a Lumonics Nd-HyperYAG laser (Nepean, ON) was used to perform LDI/LA analysis of the thin silver films with or without a gramicidin S overlayer sample. These silver films were oriented either perpendicular or parallel to the drift tube axis of the TOFMS spectrometer. The laser beam, operated at a pulse repetition rate of 1 Hz, was focused by a lens ($f = 25$ cm) to a spot size of approximately 0.3 mm in diameter on the backside of the thin silver film. The laser energy varied between 0.01 and 0.18 mJ/pulse (fwhm = 7 ns) as measured by a Scientific 365 power/energy meter equipped with a MC250 volume absorbing calorimeter (Boulder, CO). Hence, the laser fluence required for LDI/LA is approximately 14–250 mJ cm^{-2}. Consecutive laser shots ranging from 1 to 50 were summed and averaged in order to enhance the signal-to-noise quality of the resulting mass spectrum.

2.6. Surface plasmon resonance laser desorption ionization/laser ablation

The second 532 nm output of the Lumonics Nd-HyperYAG laser was used to perform SPR LDI/LA analysis of the Lumonics thin silver films with or without a gramicidin S overlayer sample and a DHB matrix. These silver films were optically coupled to a right-angle glass prism with Neovac SY diffusion pump oil to provide SPR conditions in a Kretschmann geometry [38,39]. The prism was mounted on a rotation/translation stage and oriented either perpendicular or parallel to the drift tube axis of the TOFMS spectrometer. The *p*-polarized laser beam, operated at a pulse repetition rate of 1 Hz, was focused by a lens ($f = 25$ cm) through the prism to a spot size of approxi-

mately 0.3 mm in diameter on the backside of the thin silver film. The laser energy varied between 0.01 and 0.07 mJ/pulse. Hence, the laser fluence required for SPR LDI/LA was approximately 14–100 mJ cm^{-2}. Consecutive laser shots ranging from 1 to 50 were summed and averaged in order to enhance the signal-to-noise quality of the resulting mass spectrum.

2.7. Time-of-flight mass spectrometry

All experiments were performed in a linear TOFMS spectrometer which was constructed in our laboratory [33]. The pressure inside the instrument was maintained between 2.5×10^{-7} and 1.5×10^{-6} Torr. When the silver film was oriented perpendicular to the drift tube axis, a

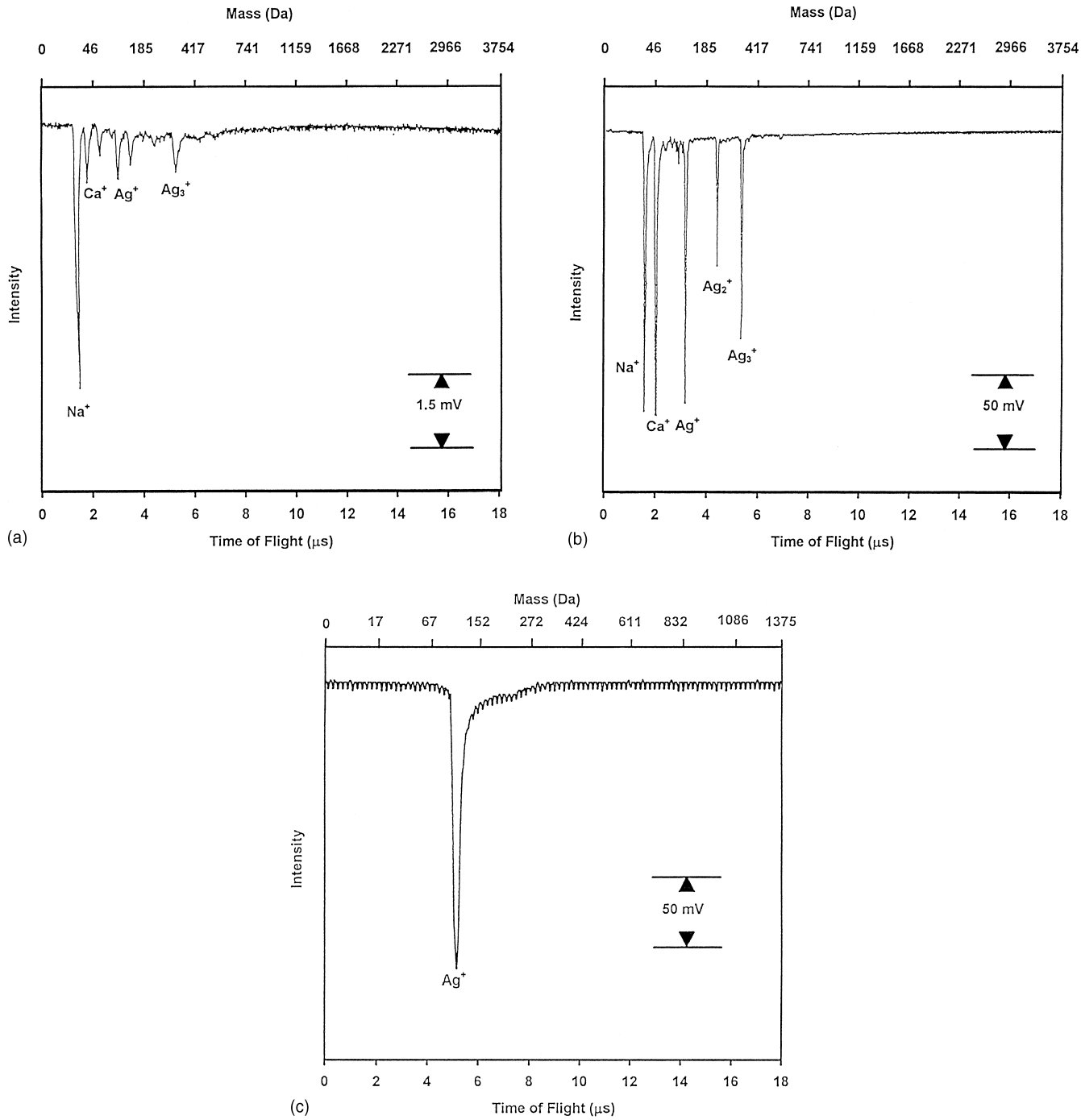

Fig. 1. LDI/LA TOFMS spectra of (a) Tollen's thin silver film in perpendicular orientation, (b) Lumonics thin silver film in perpendicular orientation and (c) Tollen's thin silver film in parallel orientation (single-shot).

+20 kV potential on the thin silver film was used to accelerate the generated cations from the source region to the field-free drift tube region. When the silver film was oriented parallel to the drift tube axis, a +20 kV potential on an aluminum repeller plate was used to achieve acceleration of the generated cations. The cations at the end of the drift tube were detected using a Comstock CP-625/50C multichannel plate detector (MCP) which consisted of dual 40 mm-diameter channelplates in a chevron configuration (Oak ridge, TN) with a front-face voltage held at −1.6 kV (gain = 5×10^4). The resulting MCP signal was fed into a 50 Ω dc-coupled 300 MHz LeCroy 9310 M digital storage oscilloscope (Chestnut Ridge, NY) or 100 MHz Gould 645 digital storage oscilloscope (Ilford, Essex, UK). A fast photodiode detector, monitoring a branch of the 532 nm output laser beam, provided prompt triggering of the oscilloscope at the onset of each laser pulse. Each laser shot yielded a single sweep, sampling ion intensities at 1024 bins on the microsecond time scale of the oscilloscope. Mass spectra were calibrated with known-mass peaks from Na^+, Ca^+, and Ag_n^+ ($n = 1$–3) using the empirical equation of $m/z = (kt)^2$ where k was a calibration constant, and t was time-of-flight observed in the mass spectrum.

3. Results

3.1. Comparison of thin Ag films

A typical sum-averaged mass spectrum of a bare Tollen's thin silver film, shown in Fig. 1(a), was acquired with the thin silver film oriented perpendicular to the drift tube axis. A large Na^+ cation signal, thought to originate from the underlying microscope glass slide, is seen in the spectrum. Also seen with this cation at somewhat lower abundances are Ag_n^+ ($n = 1,3$) cluster cation signals and a Ca^+ cation signal, also thought to originate from the slide. The signal-to-noise ratio of the Ag_n^+ cluster cation signals and Ca^+ cation signal is approximately 10 : 1, while that of the Na^+ cation signal is 30 : 1. The mass resolution ($M/\Delta M$) of 10 is more than adequate for assigning the mass spectral peaks.

A typical sum-averaged mass spectrum of a bare Lumonics thin silver film, shown in Fig. 1(b), was acquired also in a perpendicular orientation. Similar to the bare Tollen's silver film results, a large Na^+ cation signal is seen in this spectrum, accompanied with a large Ca^+ signal. Both cations are thought to originate from the underlying microscope glass slide. Also seen at slightly lower abundances are again the Ag_n^+ ($1 \leq n \leq 3$) cluster cation signals. The signal-to-noise ratio of all these cation signals is approximately 33 : 1, with a $M/\Delta M$ of 15. Comparison between the Tollen's and the Lumonics thin silver films shows a difference in mass resolution and signal intensities, most likely due to the film thickness and surface morphology, as a consequence of the silver film deposition methods, and the unique nature of back-illumination in relation to the gas-phase ion reactions described later.

A typical single-shot mass spectrum of a bare Tollens thin silver film in a parallel orientation, shown in Fig. 1(c), was acquired. Only a strong Ag^+ cation signal is observed, with a signal-to-noise ratio of 23 : 1 and $M/\Delta M$ of 10. Of primary importance is the lack of the dimer and trimer silver cluster cation signals, and the microscope slide cations generated during the ablation process. This TOFMS spectrum is identical for successive laser shots on the same spot. The signal-to-noise ratio is approximately the same as that obtained in Fig. 1(b) for the perpendicular orientation of the Lumonics thin silver film, although the resolution is considerably worse.

3.2. Various Tollen's silver film thicknesses

To determine the effectiveness of Ag^+ as a cationizing agent, different concentration ratios of silver to analyte must be analyzed. The analyte used for these experiments is gramicidin S, a cyclic decapeptide known to interact well with Ag^+ cations in the gas phase [22].

A typical sum-averaged mass spectrum of gramicidin S deposited on a Tollen's thin silver film-oriented perpendicular to the field-free drift tube axis is shown in Fig. 2. Common signals seen in both the bare and gramicidin S-deposited Tollen's thin silver film spectra are the Na^+, Ca^+, Ag^+, and Ag_3^+ cation signals. There are other signals, corresponding to larger Ag_n^+ cluster cation signals ($n \geq 4$) and small fragment ion signals of the gramicidin S analyte molecule. Notably, the gramicidin S molecular ion signal is not seen, but gramicidin S pseudomolecular ion signals, corresponding to the sodiated and 'silverated' gramicidin S molecular cations, [gramicidin S + Na]$^+$ and [gramicidin S + Ag]$^+$, are observed in the mass spectrum. Again, the peak intensities of Na^+ and Ca^+ are larger than the other mass spectral peak intensities. $M/\Delta M$ of the observed mass spectrum is 25, adequate for the assigned mass spectral peaks, with a signal-to-noise ratio of 860 : 1 for the Na^+ and Ca^+ cation signals, but a lower signal-to-noise ratio of 300 : 1 for [gramicidin S + Na]$^+$. A still lower signal-to-noise ratio of 100 : 1 is observed for [gramicidin S + Ag]$^+$.

Upon mass spectral analysis with different molecular concentration ratios of silver to gramicidin S, similar mass spectra were observed. Common cation signals observed are the Na^+, Ca^+, Ag^+, Ag_2^+, Ag_3^+, [gramicidin S + Na]$^+$ and [gramicidin S + Ag]$^+$. The Na^+ and Ca^+ cation signals are usually the most abundant, while the other cation signals are usually lower in abundance. Moreover, the abundance ratios of these cations vary randomly. Again, this may be attributed to the surface morphology, as a consequence of the silver film deposition method, and the random nature of back-illuminated silver film ablation concerning gas-phase ion reactions. Lastly, the pseudomolecular gramicidin S ions vary significantly in intensity, indicating a dependence on Tollen's silver film thickness and on laser fluence.

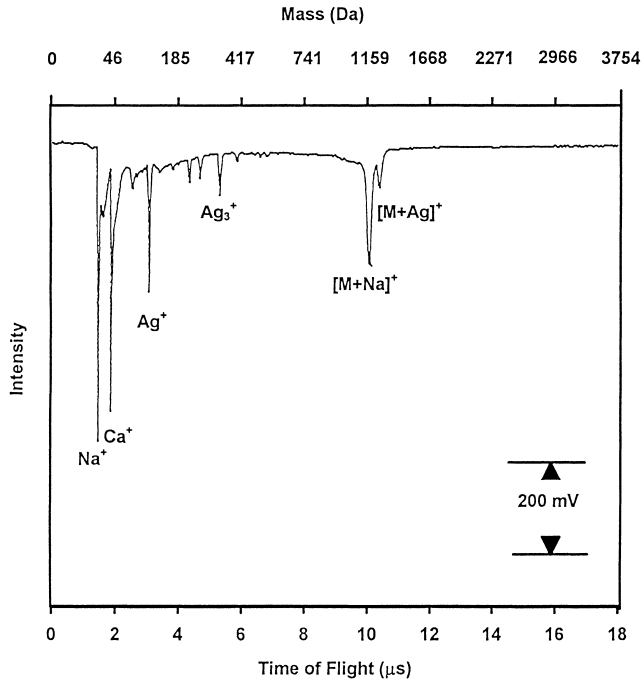

Fig. 2. LDI/TOFMS spectrum of gramicidin S deposited on Tollen's thin silver film in perpendicular orientation.

The detection of the pseudomolecular gramicidin S ion signals is of primary importance as they are the analyte of interest. Upon using higher laser fluences for laser ablation of gramicidin S on a Tollen's thin silver film of constant thickness, a change in the mass spectra occurs. As shown in Fig. 3(a–e), all common and relevant peaks are seen, but more fragmentation is apparent at the higher laser fluences. In addition, $M/\Delta M$ appears to decrease from 12.5 to 6.0 with increasing laser fluence. As the laser fluence increases, the $[\text{gramicidin S} + \text{Na}]^+$ and $[\text{gramicidin S} + \text{Ag}]^+$ signals broaden until the resolution eventually becomes so poor that the two signals overlap.

By plotting the total deconvoluted pseudomolecular gramicidin S ion signal intensity (TDIS), defined as the sum of the sodiated gramicidin S cation signal intensity and the 'silverated' gramicidin S cation signal intensity, against the incident laser energy for different Tollen's thin silver film thicknesses, shown in Fig. 4(a), a slight trend can be seen. As the Tollen's thin silver film thickness increases, the TDIS increases at first, followed by a decrease. Hence, there appears to be an optimal silver film thickness (▲) for generating a maximum TDIS (440 mV) at an optimal incident laser energy (140 μJ/pulse). Further, this trend is also seen when plotting the TDIS against the transmitted laser energy through the Tollen's thin silver film and against the absorbed laser energy by the Tollen's thin silver film. These are shown in Fig. 4(b) and (c). Although the TDIS varies with the laser fluence, the abundance ratio of the $[\text{gramicidin S} + \text{Na}]^+$ and $[\text{gramicidin S} + \text{Ag}]^+$ signals is uncorrelated with the laser fluence. Even when a constant laser energy is used, the TDIS varies for a given thin silver film thickness, hence reproducibility is somewhat limited for the same reason of random behavior as stated above.

Another important realization is the effect of the different silver film thickness on the laser beam incident on the thin silver film, transmitted through the thin silver film, and absorbed by the thin silver film. Firstly, there is an optimum incident laser energy for generating a maximum TDIS for each silver film thickness. Also, at these maximum TDIS for different film thicknesses, the incident laser energy appears to increase to a maximum value (from 70 to 175 μJ/pulse), then decrease as the thin silver film thickness increases (from 175 to 40 μJ/pulse). Secondly, plotting the TDIS against the transmitted laser energy, there also appears to be a trend (see Fig. 4(b)). At the maximum TDIS existing for different thin silver film thicknesses, the trend indicates an increase in transmitted laser energy (from 50 to 70 μJ/pulse), then a decrease in transmitted laser energy (from 70 to 5 μJ/pulse). Lastly, variations in TDIS with the absorbed laser energy by the thin silver film (see Fig. 4(c)) indicates the same trend as the incident laser energy and the transmitted laser energy plots. At the maximum TDIS existing for different thin silver film thicknesses, the laser energy absorbed by the thin silver film first increases (from 15 to 115 μJ/pulse), and then decreases (from 115 to 30 μJ/pulse).

Upon ablating gramicidin S deposited on a Tollens thin silver film oriented parallel to the field-free drift tube axis, a Ag^+ signal is produced but no gramicidin S molecular ion signal is observed in the single-shot mass spectrum shown in Fig. 5. Moreover, all of the silver dimer and silver trimer cluster cations, the microscope glass cations and pseudomolecular gramicidin S cations are absent. The observed Ag^+ signal has a $M/\Delta M$ of 13 and a signal-to-noise ratio of 18 : 1. Upon ablation with successive laser pulses, the mass spectra did not change in both the resolution and signal-to-noise. Further experiments on variations in Tollen's thin silver film thickness were not performed because the gramicidin S analyte was not detected in this orientation.

3.3. SPR LDI/LA TOFMS

Using a Lumonics thin silver film oriented perpendicular to the drift tube axis, LDI/LA TOFMS under surface plasmon resonance (SPR) conditions produces similar mass spectral peaks as the conventional LDI/LA TOFMS results for Tollen's thin silver films. A typical sum-averaged mass spectrum of a Lumonics thin silver film is shown in Fig. 6. All relevant peaks are observed. The Na^+ cation is seen at a lower abundance than the Ca^+ cation, Ag^+ cation, and the other silver cluster cations. Their abundance ratios may vary, although the Ag^+ cation usually dominates the mass spectrum. The $M/\Delta M$ is approximately 15 for the Ag^+ cation peak, while its signal-to-noise ratio of 208 : 1 is excellent. Of key importance is the low laser fluence of 33 ± 3 mJ cm^{-2} for obtaining a mass spectral signal at the SPR angle. Spectra obtained during off-resonance conditions require larger laser fluences than those obtained

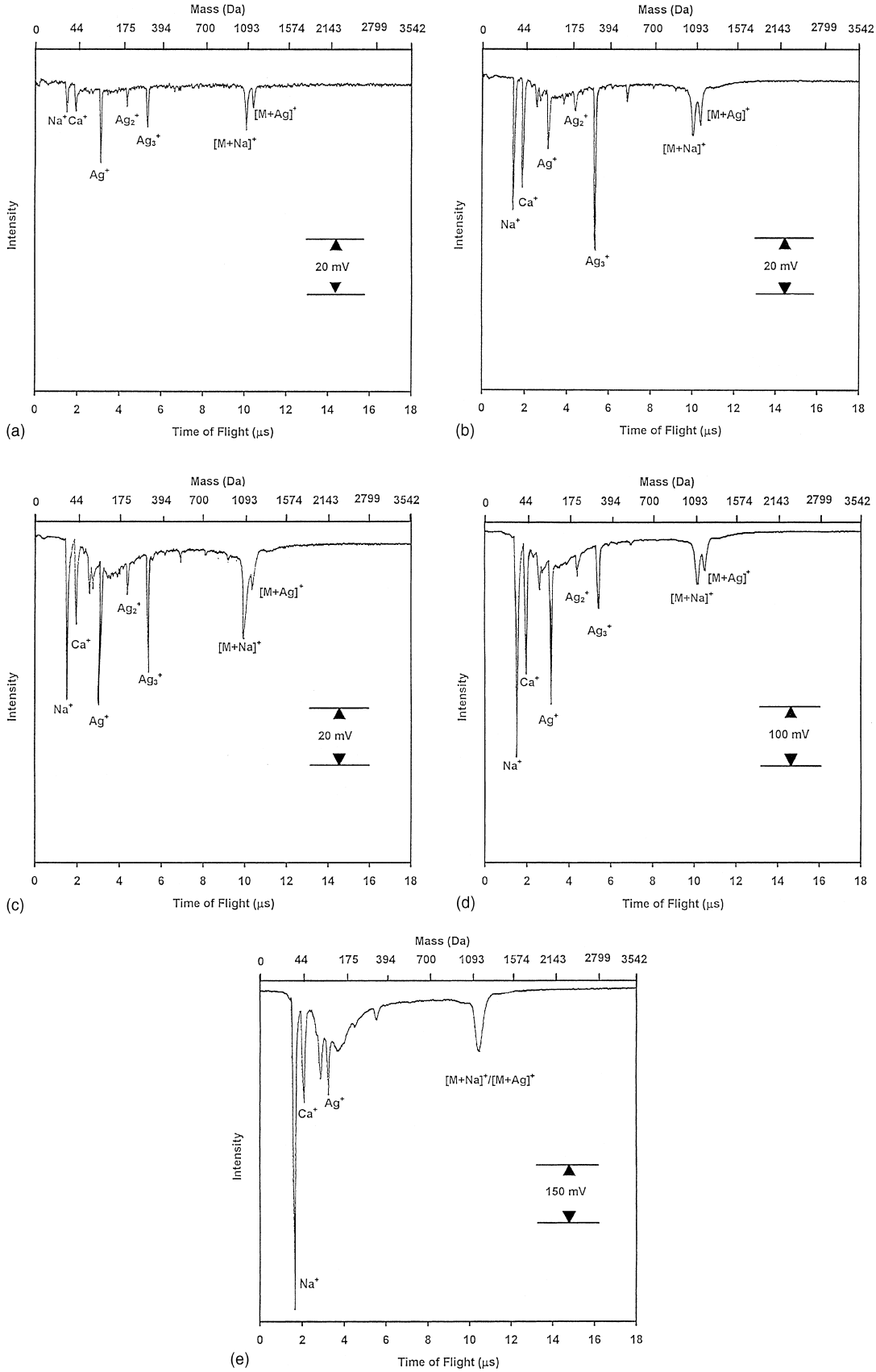

Fig. 3. LDI/LA TOFMS spectra of gramicidin S deposited on Tollen's thin silver film in perpendicular orientation using (a) 85 mJ cm^{-2}, (b) 127 mJ cm^{-2}, (c) 198 mJ cm^{-2}, (d) 240 mJ cm^{-2}, and (e) 396 mJ cm^{-2}.

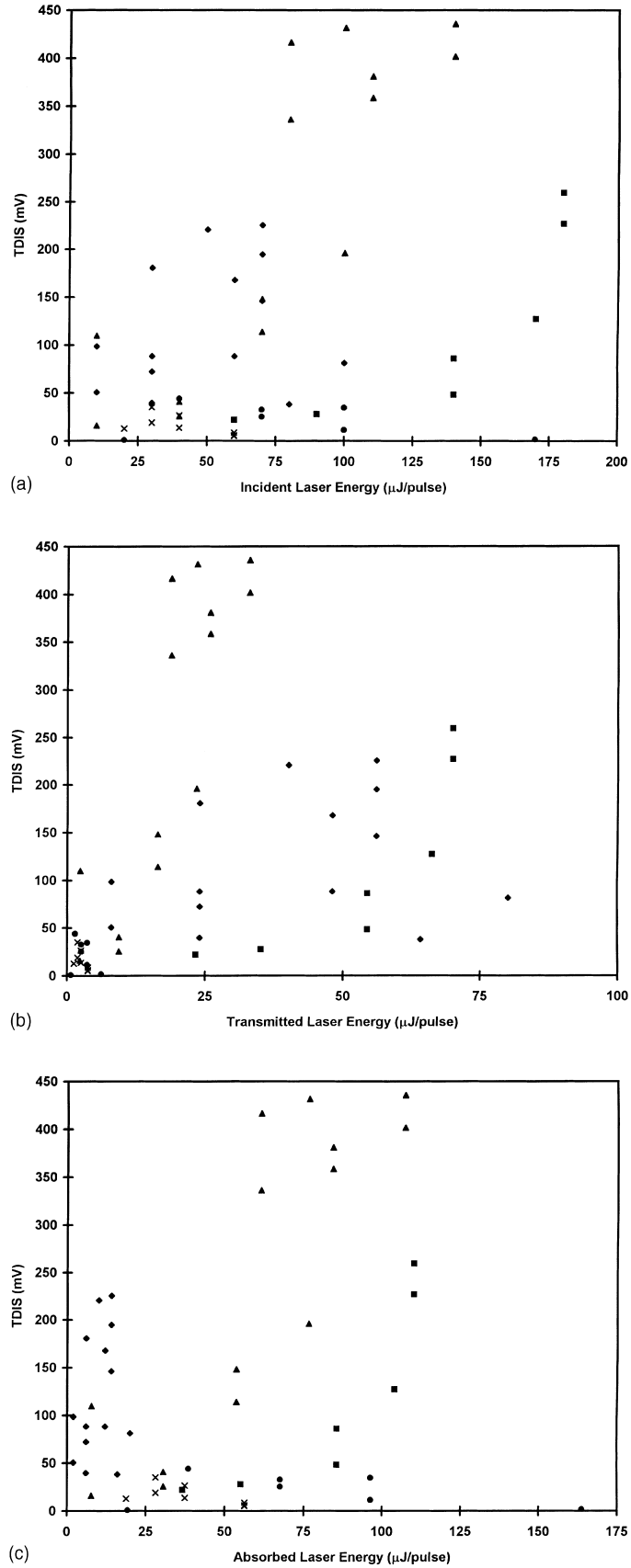

Fig. 4. TDIS dependences on (a) incident laser energy, (b) transmitted laser energy, and (c) laser energy absorbed by Tollen's thin silver films in perpendicular orientation. Spectrophotometric absorbance at 532 nm: ◆, 0.10; ■, 0.41; ▲, 0.63; ×, 1.20; ●, 1.44.

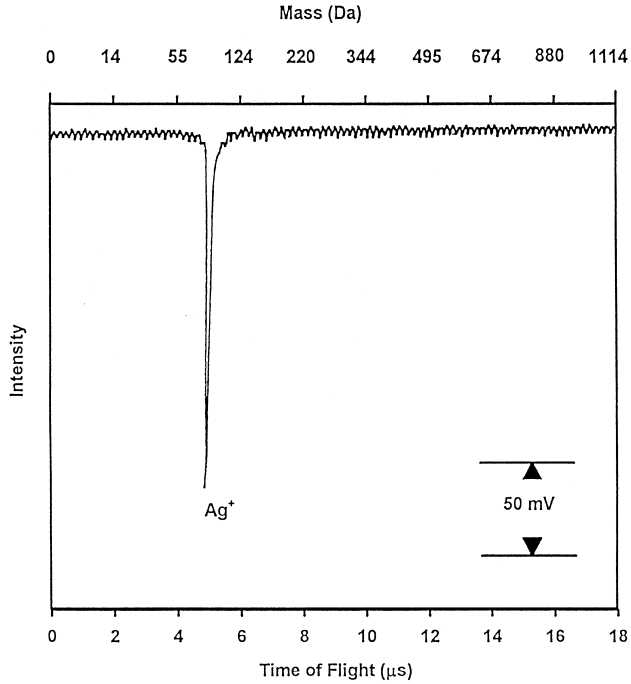

Fig. 5. LDI/LA TOFMS spectrum of gramicidin S deposited on Tollen's thin silver film in parallel orientation (single-shot).

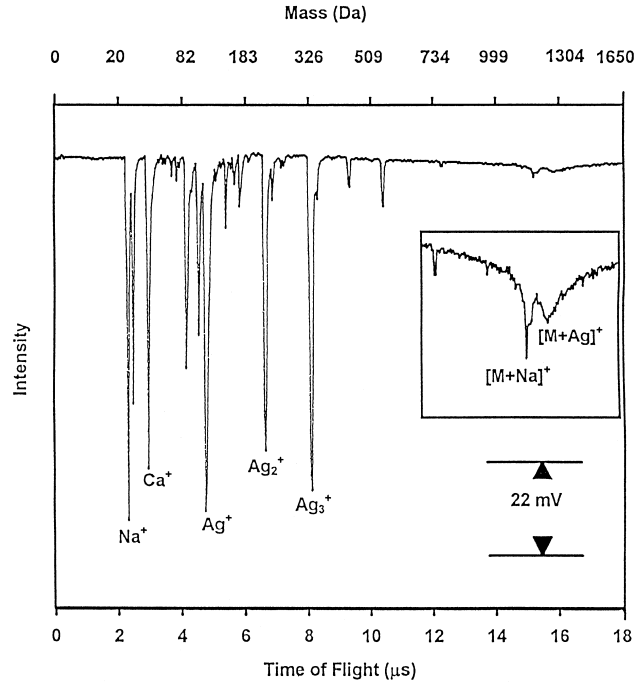

Fig. 7. SPR LDI/LA TOFMS spectrum of gramicidin S deposited on Lumonics thin silver film in perpendicular orientation.

during resonance conditions. For a constant laser fluence, a larger ablation hole accompanied with a larger abundance of cations are formed under resonance conditions.

Using a Lumonics thin silver film deposited with gramicidin S oriented perpendicular to the drift tube axis. TOFMS under SPR conditions indicates similar mass spectral peaks

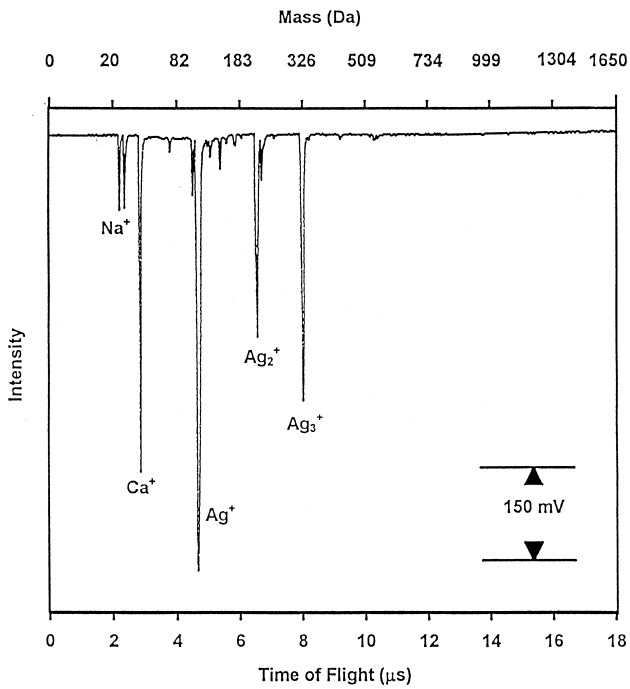

Fig. 6. SPR LDI/LA TOFMS spectrum of Lumonics thin silver film in perpendicular orientation.

as those obtained earlier from a Tollen's silver film deposited with gramicidin S. A typical sum-averaged mass spectrum is shown in Fig. 7. The most abundant peaks are the Na^+, Ca^+ and Ag_n^+ cluster cation signals, while lower abundances are exhibited by the [gramicidin S + Na]$^+$ and [gramicidin S + Ag]$^+$ signals. The $M/\Delta M$ is 12 while the signal-to-noise ratio is approximately 10 : 1 and 5 : 1 for the pseudomolecular gramicidin S ions. Again, a laser fluence of approximately 55 mJ cm^{-2} is required for ablation at the SPR angle, which is higher than that for a Lumonics thin silver film at its own SPR angle, and which is lower than those required under off-resonance conditions. At constant laser fluence, a larger abundance of gramicidin S signals is seen under resonance conditions than off-resonance conditions. Fragmentation ion signals are also observed, with *m/z* values ranging from 88 to 200.

Gramicidin S mixed with a commonly-used MALDI matrix, 2,5-dihydroxybenzoic acid (DHB), is analyzed on a Lumonics thin silver film using the back-illuminated SPR LDI/LA TOFMS technique. All relevant ion signals are present in the sum-averaged mass spectrum, including [gramicidin S + Na]$^+$ but not [gramicidin S + Ag]$^+$, as shown in Fig. 8. Hence, it appears as if the matrix hinders the production of [gramicidin S + Ag]$^+$. This may be regarded as an advantage in terms of simpler mass spectral interpretation. The $M/\Delta M$ is approximately 12 while the signal-to-noise ratio is approximately 10 : 1 for the [gramicidin S + Na]$^+$ ion. More importantly, the laser fluence required to generate any cation signal is 30 ± 10 mJ cm^{-2}, which is roughly the same as that required for a Lumonics thin silver film. Hence, the SPR LDI/LA event happens with a lower

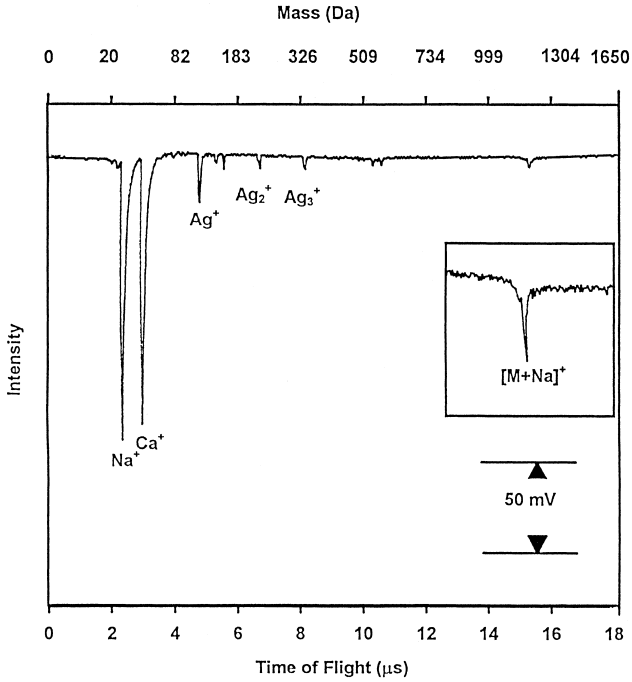

Fig. 8. SPR LDI/LA TOFMS spectrum of gramicidin S with DHB matrix deposited on Lumonics thin silver film in perpendicular orientation.

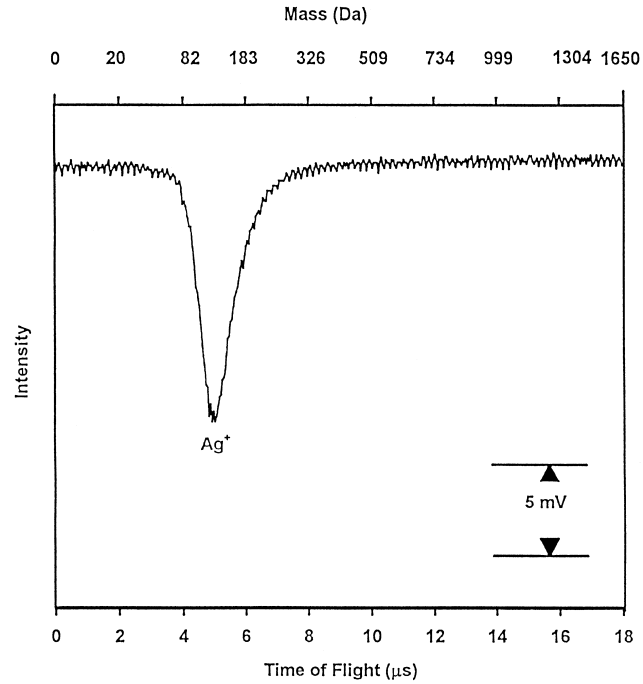

Fig. 9. SPR LDI/LA TOFMS spectrum of Lumonics thin silver film in parallel orientation (single-shot).

fluence requirement than LDI. The addition of a matrix desorbs all the gramicidin S from the silver film surface, leaving no gramicidin S remaining on the silver film surface after the ablation irrespective of the angle of laser incidence. Fragmentation ions from the gramicidin S and DHB are also observed in the mass spectrum. Again, the [gramicidin S + Na]$^+$ and [gramicidin S + Ag]$^+$ abundance ratio varies randomly with analyte/matrix composition and angle of laser incidence. Upon closer examination of all the SPR LDI/LA TOFMS spectra, the higher Ag_n^+ cluster cations ($n \geq 4$) seem to appear when an ablation hole begins to form. There does not seem to be any correlation between the highest Ag_n^+ cluster cations ($n \geq 4$) appearing and the angle of laser incidence. However, a correlation exists between the laser fluence required and the angle of laser incidence to generate the higher Ag_n^+ cluster cations ($n \geq 4$).

A typical single-shot mass spectrum obtained for a Lumonics thin silver film under SPR conditions, with the sample oriented parallel to the drift tube axis, differs significantly from those obtained above in the perpendicular orientation. As shown in Fig. 9, a broad peak signal is observed with a $M/\Delta M$ of two which is inadequate for specific mass assignment. Only when other results are used for comparison can this peak (with a signal-to-noise ratio of 18 : 1) be assigned as the Ag^+ signal. In addition, the resolution does not appear to change with the angle of laser incidence. It is also important to realize the absence of higher Ag_n^+ cation peaks. A lower laser fluence is always sufficient for generating a mass spectrum at the SPR angle. Fig. 10 shows a typical single-shot SPR LDI/LA TOFMS spectrum for gramicidin S deposited on a Lumonics thin silver film oriented parallel to the drift tube axis. The same Ag^+ cation peak signal is observed with a $M/\Delta M$ of two and a signal-to-noise ratio of 18 : 1, which does not change with variations in angle of laser incidence. Again, a lower laser fluence can always generate a mass spectrum at the SPR angle. The lowest laser fluence required to generate a SPR LDI/LA TOFMS spec-

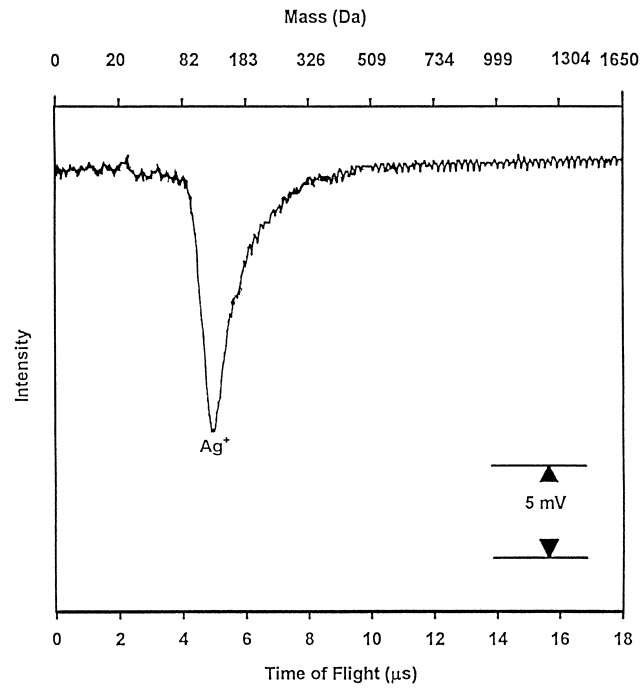

Fig. 10. SPR LDI/LA TOFMS spectrum of gramicidin S deposited on Lumonics thin silver film in parallel orientation (single-shot).

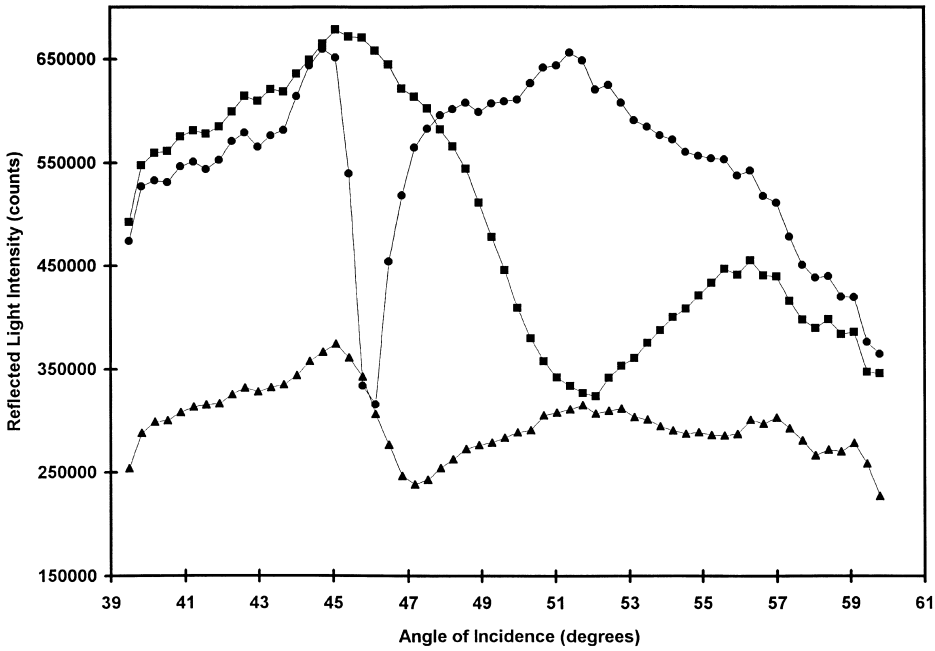

Fig. 11. SPR angular profiles of Lumonics thin silver film (●), gramicidin S deposited on Lumonics thin silver film (■), and gramicidin S with DHB matrix deposited on Lumonics thin silver film (▲).

trum corresponds with a dip in reflectance at the SPR angle, as shown in Fig. 11 for various silver/DHB/gramicidin S combinations. Previous reports by Lee et al. using a thin aluminum film to desorb rhodamine B also indicated enhanced desorption by SPR, accompanied with a lower laser fluence requirement at the SPR angle [31,32].

4. Discussion

The LDI/LA mechanisms involved in this study can be simply put into two categories: (a) ions directly desorbed from the thin silver film, and (b) CI. These mechanisms play a role in the generation of specific mass spectral species, as supported by various experimental results described above. The orientation of the different types of thin silver film dictates the production of different mass spectra. However, there does not seem to be any correlation among the signal-to-noise ratios for all the different cationic species observed in the mass spectra. Also, the production of different mass spectral species is not effected by the addition of SPR excitation. Hence, the thin silver film thickness and the absorbance of *p*-polarized laser light at the SPR angle do not play a role in which specific mass spectral species will be generated. These major observations will be discussed below in detail.

With or without SPR conditions, the thin silver film oriented parallel to the drift tube axis only produces the Ag^+ monomer cation. Hence, this cation is most likely directly desorbed as a consequence of the thin silver film absorbing the incident laser energy. More interestingly, when the thin silver film is oriented perpendicular to the drift tube axis, the production of Ag_n^+ clusters cations and pseudomolecular gramicidin S cations is evident. This suggests that gas-phase ion reactions must occur between the directly desorbed Ag^+ monomer cations and the neutral silver atoms/clusters or gramicidin S molecules within the ablation plume:

$$Ag_{n-1} + Ag^+ \rightarrow Ag_n^+$$

$$\text{gramicidin S} + Ag^+ \rightarrow [\text{gramicidin S} + Ag]^+$$

Since the spectra are measured at 1 Hz, this means that the Ag^+ monomer cation is not entirely produced at the thin silver film surface, else these gas-phase ion reactions would not be able to occur efficiently. Gramicidin S molecules are introduced to the ablation plume after the silver film decomposes under laser irradiation so that the film surface for adsorption of the gramicidin S molecules disappears.

When a potential is applied to either type of thin silver films oriented perpendicular to the drift tube axis, the Na^+, Ca^+, and Ag^+ cations are present within the ablation plume in addition to neutral atoms/clusters [40]. These cations travel through the ablation plume along the drift tube axis as illustrated in Fig. 12(a), thereby increasing gas-phase ion/molecule reaction probability (higher cross-section). These reactions are responsible for the production of the Ag_n^+ cluster cations and the pseudomolecular gramicidin S cations. However, upon ablation of a thin silver film oriented parallel to the drift tube axis, the generated Ag^+ cations must travel perpendicular to and therefore away from the ablation plume (also shown in Fig. 12(b)). Hence, no significant interaction with the neutrals can occur, resulting in a lower probability of gas-phase ion/molecule reactions.

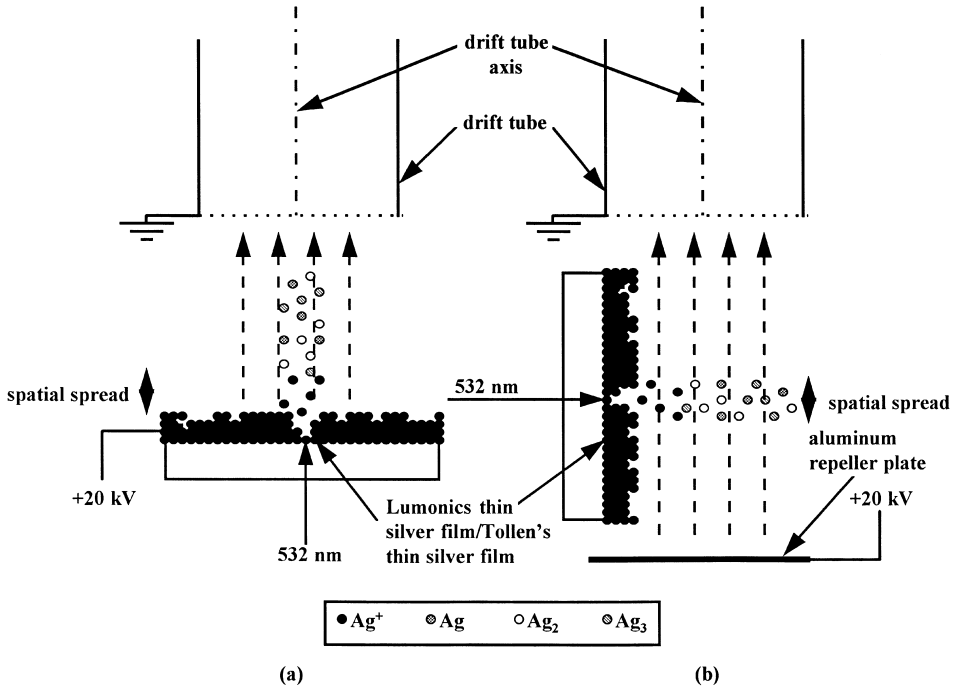

Fig. 12. Production of Ag^+ monomeric cations and neutral Ag_n atoms/clusters in ablation plume with the thin silver films in (a) perpendicular orientation, and (b) parallel orientation.

Abundant Ag_n^+ cluster cations are generated immediately from a Tollen's thin silver film in all LDI/LA experiments. Generation of the Ag_n^+ cluster cations in abundance, however, only occurs upon visible formation of an ablation hole in a Lumonics thin silver film. Hence, a difference in surface morphology between the two types of thin silver films may attribute to the production of neutral Ag_n atoms and clusters which can undergo gas-phase ion/molecule reactions. Generally, atoms and clusters are more likely to desorb when the surface is not uniform. Hence, their production from the Tollen's thin silver film surface may be more favourable than from the Lumonics thin silver film. The efficiency of gas-phase ion/molecule reactions may greatly vary, resulting in large fluctuations of the Ag_n^+ cluster cation and pseudomolecular gramicidin S ion abundances.

Other research groups have previously suggested that the probability of Ag_n^+ cluster cation generation during FAB experiments increases with increasing temperature [41,42]. However, the generation of cluster cations in the present LDI/LA experiments does not appear to correlate with the laser fluence (and hence temperature). Our investigation into the LDI/LA mechanism indicates an electronic excitation process followed by a thermal desorption step. It has previously been suggested that the silver clusters on a glass plate absorb laser light to excite surface plasmon modes of electrons in the clusters [43]. The electronically excited silver surface plasmon mode then loses energy by transferring it to surface clusters and absorbed analyte molecules. This is supported by the pseudomolecular gramicidin S cation signal which evolves from an initial narrow peak (by electronic excitation) into a final broader one (by thermal desorption) as the laser fluence is increased [44]. According to the one-dimensional model, the thin silver film's backside temperature eventually increases to 900 ± 200 K [45,46], which comes very close to the melting point of silver. The possibility of film melting at high laser fluences during LDI/LA has been discussed in previous reports, which indicate that the melting process may affect a variable fraction of the total thickness of the thin film [47]. Since thermal conductance varies with distance from the thin silver film backside to the film surface, different silver film thicknesses should yield varying pseudomolecular gramicidin S cation intensities. As the silver film thickness increases, more energy must be supplied on the film backside to desorb gramicidin S neutral molecules off the film surface. Hence, the incident laser energy required for generating a narrow pseudomolecular gramicidin S cation signal is a consequence of an electronic excitation mechanism, followed by subsequent gas-phase ion/molecule reactions. Higher laser energies generate broader pseudomolecular gramicidin S cation signals due to the additional thermal desorption step and subsequent gas-phase reaction. Based on the TDIS results, as the silver film thickness increases, electronic excitation becomes less efficient and the thermal desorption step begins to dominate. Hence, the incident laser energy must be controlled at a sufficiently low level to obtain TDIS signals due to electronic excitation only for plotting in Fig. 4(a–c).

The resolution of a TOFMS spectrum can reveal the LDI/LA energetics, including those for the present SPR mechanism. The resolutions obtained from a Tollen's thin silver film and a Lumonics thin silver film (oriented perpendicular and

parallel to the drift tube axis) are in good agreement with one another, suggesting similar LDI/LA energetics. Comparable resolutions are also obtained from gramicidin S deposited on these two types of thin silver films. Hence, a general LDI/LA process may be applied to all film/matrix/analyte-combinations. On the contrary, the energy dissipated from a Lumonics thin silver film backside to the film surface is different under SPR conditions. It is speculated that the Lumonics thin silver film absorbs the laser energy via SPR excitation and next transfers this energy to vibronic modes on the thin silver film surface to enhance desorption/ablation, thus, lowering the laser fluence requirement [31–33]. Furthermore, under SPR conditions a Lumonics thin silver film oriented parallel to the drift tube axis gives a much poorer resolution than a Lumonics thin silver film oriented perpendicular to the drift axis. Apparently, absorption of *p*-polarized laser light by the Lumonics thin silver film in the parallel orientation increases the spatial and kinetic energy distributions of the Ag^+ monomer cations and neutrals generated within the ablation plume as shown in Fig. 13(a). When ablating the Lumonics thin silver film in the perpendicular orientation, the spatial and kinetic energy distributions along the drift tube axis are relatively small as illustrated in Fig. 13(b). Hence, the perpendicular orientation is able to afford better resolution as well as a higher gas-phase ion/molecule reaction probability. Subsequently, various cations are generated through CI with Na^+ and Ag^+ cations, as shown in Fig. 7.

The ability to obtain highly-resolved TDIS under SPR LDI/LA conditions again indicates an electronic excitation mechanism without significant thermal peak broadening. The absorbance of the Lumonics thin silver film is 1.22, which requires a minimum laser fluence of approximately 55 mJ cm^{-2} to produce a SPR LDI/LA mass spectrum. According to earlier LDI/LA mass spectral results for Tollen's thin silver films, TDIS could be obtained from a film of 1.22 absorbance up to a laser fluence of 85 mJ cm^{-2} beyond which a thermal mechanism begins to dominate. Since a fluence of only 55 mJ cm^{-2} is used to obtain TDIS under SPR LDI/LA conditions, the electronic excitation mechanism must be responsible.

Upon addition of the DHB matrix compound, an even lower laser fluence (approximately 30 mJ cm^{-2}) is required for the SPR LDI/LA of gramicidin S. This can be explained by the fact that these gramicidin S molecules are isolated in the matrix and not directly associated with each other or adsorbed to the Lumonics thin silver film surface. Hence, less heat of desorption ($\Delta H_{desorption}$) is involved. Note that the SPR angular profile observed for the gramicidin S with DHB is only slightly shifted from that for a bare Lumonics thin silver film, suggesting that few gramicidin S molecules are adsorbed to the film surface in the presence of the DHB matrix. Consequently, larger quantities of gramicidin S on the film surface undergo SPR LDI/LA in the first several laser pulses along with the matrix. The desorbed matrix further hinders the CI between the Ag^+ monomer cations and gramicidin S neutrals, resulting in maximal formation of sodiated gramicidin S cations. The low requirement in laser fluence, the large quantity of desorption and the maximal amount of sodiation are all beneficial factors for the mass analysis of gramicidin S by the SPR LDI/LA technique. This is the first result which confirms the physical function of matrix isolation in LDI/LA, without the photoexcitation aspect since DHB does not serve as a chromophore to

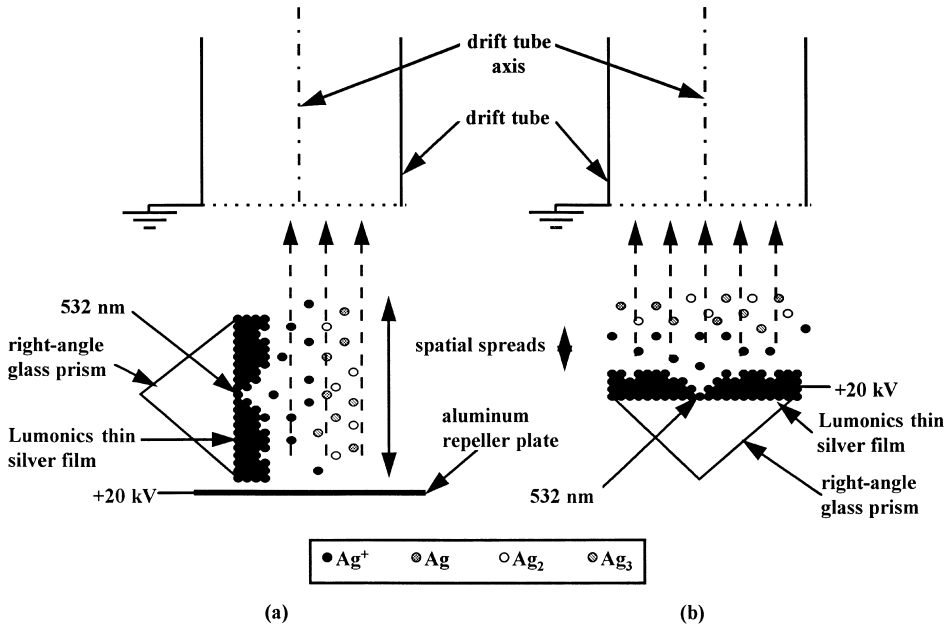

Fig. 13. Production of Ag^+ monomeric cations and neutral Ag_n atoms/clusters in ablation plume under SPR excitation with the thin silver films in (a) parallel orientation, and (b) perpendicular orientation.

absorb the 532 nm laser light in the present SPR excitation technique.

5. Conclusion

The present LDI/LA TOFMS of thin silver films demonstrates that the Ag^+ monomer cation and neutrals are generated through an electronic excitation desorption mechanism. Silver films of different surface morphologies dictate the abundance and rate of neutral silver cluster formations. These clusters undergo CI with Ag^+ monomer cations in the gas-phase to produce Ag_n^+ cluster cations. Upon LDI/LA of gramicidin S from the film surface, CI of the cyclic decapeptide with the Ag^+ and/or Na^+ cations forms both the silverated and sodiated molecular cations. An electronic excitation desorption mechanism is responsible for the TDIS, which is observed in great abundance at an optimal silver film thickness. The use of larger laser fluences results in additional thermal desorption. Under SPR conditions, a significant decrease in laser fluence requirement is observed for the appearance of TDIS. The addition of a matrix hinders the CI between Ag^+ monomer cations and gramicidin S neutrals, and offers an even lower laser fluence requirement for the abundant formation of sodiated gramicidin S cations. These factors are all beneficial for the mass analysis of gramicidin S by the SPR LDI/LA technique in the presence of a matrix. Research is continued in our laboratory to further develop this new technique for biomolecules of higher masses.

Acknowledgements

This research program was supported by the Natural Sciences and Engineering Research Council of Canada. We would also like to thank A.D.O. Bawagan, Michel Grenier and Jim Logan for assistance in construction of the TOFMS instrument.

References

[1] J.P. Speir, I.J. Amster, Anal. Chem. 64 (1992) 1041–1046.
[2] T. Hertel, M. Wolf, G. Ertl, J. Chem. Phys. 102 (1995) 3414.
[3] R.S. Mackay, K.H. Junker, J.M. White, J. Vac. Sci. Technol. A 12 (1994) 2293.
[4] A.M. Bonch-Bruevich, T.A. Vartanyan, Y.N. Maksimov, S.G. Przhibel'skii, V.V. Khromov, Surf. Sci. 307–309 (1994) 350.
[5] J. Siegel, K. Ettrich, E. Welsch, E. Matthias, Appl. Phys. A 64 (1997) 213–218.
[6] A. Rosenfeld, E.E.B. Campbell, Appl. Surf. Sci. 96–98 (1996) 439.
[7] S. Preuss, E. Matthias, M. Stuke, Appl. Phys. A 59 (1994) 79.
[8] E. Matthias, M. Reichling, J. Siegel, O.W. Kading, S. Petzoldt, H. Skurk, P. Bizenberger, E. Neske, Appl. Phys. A 58 (1994) 129–136.
[9] T. Gotz, M. Bergt, W. Hoheisel, F. Trager, M. Stuke, Appl. Phys. A 63 (1996) 315–320.
[10] J.T. Dickinson, S.C. Langford, J.J. Shin, D.L. Doering, Phys. Rev. Lett. 73 (1994) 2630.
[11] W. Hoheisel, M. Vollmer, F. Trager, Phys. Rev. B 48 (1993) 17463.
[12] K. Hattori, A. Okano, Y. Nakai, N. Itoh, R.F. Haglund Jr., , J. Phys.: Condens. Matter 3 (1991) 1001.
[13] M. Vollmer, F. Trager, Surf. Sci. 187 (1987) 445.
[14] N. Nishi, H. Shinohara, T. Okuyama, J. Chem. Phys. 80 (1984) 3898.
[15] Q. Zhan, S.J. Wright, R. Zenobi, J. Am. Soc. Mass Spectrom. 8 (1997) 525–531.
[16] A. Bjarnason, Anal. Chem. 68 (1996) 3882–3883.
[17] S. Geribaldi, S. Breton, M. Decouzon, M. Azzaro, J. Am. Soc. Mass Spectrom. 7 (1996) 1151–1160.
[18] Q.P. Lei, I.J. Amster, J. Am. Soc. Mass Spectrom. 7 (1996) 722–730.
[19] H.F. Wu, J.S. Brodbelt, J. Am. Chem. Soc. 116 (1994) 6418–6426.
[20] E.F. Cromwell, K. Reihs, M.S. de Vries, S. Ghaderi, H.R. Wendt, H.E. Hunziker, J. Phys. Chem. 97 (1993) 4720–4728.
[21] B.H. Wang, K. Dreisewerd, U. Bahr, M. Karas, F. Hillenkamp, J. Am. Soc. Mass Spectrom. 4 (1993) 393–398.
[22] E.P.C. Lai, S. Owega, R. Kulczycki, J. Mass Spectrom. 33 (1998) 554–564.
[23] A. Hachimi, J.F. Muller, Chem. Phys. Lett. 268 (1997) 485–492.
[24] C.G. Gill, A.W. Garrett, A.W. Earl, N.S. Nogar, P.H. Hemberger, J. Am. Soc. Mass Spectrom. 8 (1997) 718–723.
[25] F. Bouchard, V. Brenner, C. Carra, J.W. Hepburn, G.K. Koyanagi, T.B. McMahon, G. Ohanessian, M. Peschke, J. Phys. Chem. A 101 (1997) 5885–5894.
[26] C.G. Gill, A.W. Garrett, P.H. Hemberger, N.S. Nogar, J. Am. Soc. Mass Spectrom. 7 (1996) 664–667.
[27] I.G. Dance, K.J. Fisher, G.D. Willett, Inorg. Chem. 35 (1996) 4177–4184.
[28] T. Gotz, M. Bergt, W. Hoheisel, F. Trager, M. Stuke, Appl. Surf. Sci. 96–98 (1996) 280–286.
[29] J.K. Gibson, J. Fluorine Chem. 78 (1996) 65–74.
[30] A. Hachimi, E. Poitevin, G. Krier, J.F. Muller, M. Ruiz-Lopez, Int. J. Mass Spectrom. Ion Process. 144 (1995) 23.
[31] I. Lee, T.A. Callcott, E.T. Arakawa, Anal. Chem. 64 (1992) 476–478.
[32] I. Lee, T.A. Callcott, E.T. Arakawa, Phys. Rev. B 47 (1993) 6661–6666.
[33] S. Owega, E.P.C. Lai, A.D.O. Bawagan, Anal. Chem. 70 (1998) 2360–2365.
[34] P. Dawson, G. Cairns, J. Modern Optics 41 (1994) 1287–1294.
[35] E.T.P. Sze, T.W.D. Chan, G. Wang, J. Am. Soc. Mass Spectrom. 9 (1998) 166–174.
[36] K. Dreisewerd, M. Schurenberg, M. Karas, F. Hillenkamp, Int. J. Mass Spectrom. Ion Process. 141 (1995) 127–148.
[37] R.T. McIver, Y. Li, R.L. Hunter, Int. J. Mass Spectrom. Ion Process. 132 (1994) L1–L7.
[38] Z.E. Kretschmann, Physics 241 (1971) 313–324.
[39] V.A. VanderNoot, E.P.C. Lai, Spectroscopy 6 (1991) 28–33.
[40] R.F. Haglund, Jr., Appl. Surf. Sci. 96–98 (1996) 1–13.
[41] J. Summer, A. Morales, P. Kebarle, Int. J. Mass Spectrom. Ion Process. 87 (1989) 287.
[42] G. Szekely, J. Allison, J. Am. Soc. Mass Spectrom. 8 (1997) 337–351.
[43] H.S. Kim, T.D. Wood, A.G. Marshall, J.Y. Lee, Chem. Phys. Lett. 224 (1994) 589–594.
[44] M. Handschuh, S. Nettesheim, R. Zenobi, J. Chem. Phys. 107 (1997) 2603–2610.
[45] S. Nishigaki, W. Drachsel, J.H. Block, Surf. Sci. 87 (1979) 389–409.
[46] J.F. Ready, Effects of High Power Laser Radiation, Academic Press, New York, 1971, p. 73.
[47] Z. Toth, B. Hopp, Z. Kantor, F. Ignacz, T. Szorenyi, Z. Bor, Appl. Phys. A 60 (1995) 431–436.